Brucella abortus induces a Warburg shift in host metabolism that enhances intracellular replication of the pathogen

Daniel M. Czyż[a,b], Jonathan Willett[a,b], Sean Crosson[a,b,c#]

Howard Taylor Ricketts Laboratory, University of Chicago, Argonne National Laboratory, Lemont, Illinois, USA[a]; Department of Biochemistry and Molecular Biology, University of Chicago, Chicago, Illinois, USA[b]; Department of Microbiology, University of Chicago, Chicago, Illinois, USA[c]

Running title: *Brucella abortus* infection and host cell metabolism

[#]Address correspondence to Sean Crosson, scrosson@uchicago.edu

KEYWORDS: Metabolism, Warburg effect, lactate, Brucella, therapeutics

ABSTRACT

Intracellular bacterial pathogens exploit host cell resources to replicate and survive inside the host. Targeting these host systems is one promising approach to developing novel antimicrobials for intracellular infections. We show that human macrophage-like cells infected with *Brucella abortus* undergo a metabolic shift characterized by attenuated tricarboxylic acid cycle metabolism, altered mitochondrial morphology and increased lactate production. This shift to an aerobic glycolytic state resembles the Warburg effect, a change in energy production that is well-described in cancer cells, and also occurs in activated inflammatory cells. *B. abortus* efficiently uses lactic acid as a carbon and energy source and requires the ability to metabolize lactate for normal replication in human macrophage-like cells. We further demonstrate that chemical inhibitors of host glycolysis and lactate production do not affect *in vitro* growth of *B. abortus* in axenic culture, but decrease its replication in the intracellular niche. Our data support a model in which infection shifts host metabolism to a Warburg-like state, and *B. abortus* uses this change in metabolism to promote intracellular replication. Pharmacological perturbation of these features of host cell metabolism may be a useful strategy to inhibit infection by intracellular pathogens.

IMPORTANCE

Brucella spp. are intracellular pathogens that cause disease in a range of mammals, including livestock. Transmission from livestock to humans is common and can lead to chronic human disease. Human macrophage-like cells infected with *Brucella abortus* undergo a Warburg-like metabolic shift to an aerobic glycolytic state that produces lactic acid, which *B. abortus* can use as a carbon and energy source to promote its growth.

We provide evidence that the pathogen exploits this change in host metabolism to replicate in the intracellular niche. Drugs that target this feature of host cell metabolism inhibit intracellular replication of *B. abortus* and may be broadly useful therapeutics for intracellular infections.

INTRODUCTION

Macrophages can be activated by pathogen-associated pro-inflammatory molecules such as lipopolysaccharide (LPS). Classically activated (i.e. M1) macrophages undergo a major metabolic shift in which the tricarboxylic acid (TCA) cycle is downregulated, and energy production transitions from oxidative phosphorylation to the less efficient process of aerobic glycolysis (1, 2). This change in metabolism, known as the Warburg effect (3), is a well-described metabolic feature of cancer cells (4). Increased glucose consumption through glycolysis is thought to increase adenosine triphosphate (ATP) levels; a corresponding increase in pentose phosphate pathway activity generates nicotinamide adenine dinucleotide phosphate (NADPH), which is subsequently used by NADPH oxidases to generate reactive oxygen species (ROS) (5). This metabolic shift is important in enabling cells to launch general antimicrobial defense mechanisms by increasing concentrations of ROS and reactive nitrogen intermediates (6).

The intracellular pathogen *Brucella abortus* invades host cells and is trafficked to a compartment known as the Brucella containing vacuole, where it replicates. To successfully find its way to this niche, *B. abortus* must avoid numerous chemical insults by the host cell and adapt to the nutrient resources available within the host. The

mechanisms by which *B. abortus* evades host defenses and takes advantage of host metabolic responses remain understudied. *B. abortus* induces a Warburg-like effect in mammalian host cells. We demonstrate that this metabolic shift is advantageous for *B. abortus* replication, and that chemical inhibition of Warburg metabolism in macrophage-like cells attenuates intracellular replication of *B. abortus*. Thus, *B. abortus* exploits an innate immune metabolic response to support infection.

RESULTS

Brucella abortus infection of human macrophage-like cells disrupts mitochondrial function and morphology

To characterize the effect of intracellular colonization by *B. abortus* on human cell metabolism, we employed mammalian cell phenotype microarrays (PM) to measure respiration in terminally differentiated, metabolically active THP-1 cells. These cells were cultivated in minimal essential medium in the presence of central metabolic substrates specifically selected to measure mitochondrial function. Three of the substrates, α-ketoglutaric acid, β-hydroxybutyric acid, and pyruvic acid are metabolized in mitochondria. We assessed the respiration of the human cells solely utilizing the provided substrate as a primary energy source by colorimetrically measuring reduction of a redox indicator dye. This assay allows us to assess the cells' ability to metabolize substrates across different molecular pathways, and thus provides a measurement of metabolic pathway activity upon infection (Figure 1A). We infected the cells with *B. abortus* at increasing multiplicities of infection (MOI). To eliminate the possibility that

changes in the metabolic activity of human cells are caused by *Brucella*-induced cell death, we removed medium containing mitochondrial substrates and replaced it with a regular growth medium containing glucose, followed by assessment of cell viability using the MTT (3-(4,5-dimethylthiazol-2-yl)-2,5-diphenyltetrazolium bromide) assay. The number of viable cells remained the same at different *Brucella* MOI (Figure 1B). Naïve cells utilized all of the mitochondrial substrates (Figure 1C), but their ability to utilize those substrates decreased in cells infected with *B. abortus* (Figure 1D). This decrease was dependent on MOI (Figures 1A). *Brucella*-infected cells, unlike with all other substrates, continued to utilize glucose (Figure 1C–D). In fact, infected cells increased glucose consumption with increasing MOI (Fig. S1).

The marked inhibition of mitochondrial substrate utilization suggests that intracellular Brucellae diminish mitochondrial function. Parasites (7), viruses (8), and intracellular bacterial pathogens including *B. melitensis* (9) and *Listeria monocytogenes* (10) perturb mitochondrial function in host cells. To obtain additional evidence that mitochondrial function is disrupted during *B. abortus* infection, we examined mitochondrial morphology in uninfected and infected HeLa cells (because THP-1 cells are not amenable to mitochondrial staining or imaging). Disruptions of mitochondrial structure were observed in HeLa cells with detectable *B. abortus*, whereas uninfected cells in the same field of view had normal cellular and mitochondrial morphology (Figure 2). Using an MTT cell viability assay we detected no loss in host viability with increasing MOI within the same timeframe (Figure 1B). Therefore, it is unlikely that the mitochondrial disruption observed by fluorescence microscopy results from host cell death.

Most amino acids can be metabolized to enter the TCA cycle through anaplerotic reactions (11). To determine whether the observed *B. abortus*-mediated disruption of host mitochondrial function directly affects amino acid metabolism, we assessed the effect of infection on the host's ability to utilize amino acids as a carbon source. While glucose metabolism was unaffected, infected cells could not metabolize any of the amino acids known to enter the TCA cycle (Figure 3). Together, the results of these experiments are consistent with a model in which infection of human macrophages with *B. abortus* results in major metabolic changes that are linked to disruption of mitochondrial function.

***Brucella*-dependent induction of lactic acid production in human cells**

Macrophages and dendritic cells are central to innate immunity. Upon activation, they can undergo a shift in energy metabolism by shutting down oxidative phosphorylation and increasing the rate of aerobic glycolysis in a process known as the Warburg effect (3). A hallmark of this effect is production of lactic acid in the presence of oxygen. An increase in lactate production in non-polarized macrophages infected with *Brucella* spp. has been previously noted (12). To further validate that THP-1 infected with *B. abortus*-are shifted toward a Warburg-like state, we measured the production of lactic acid in host cells as a function of increasing MOI. THP-1 cells increase lactic acid production in an MOI-dependent manner (Figure 4A). These results, together with the data presented in Figures 1-3 support a model in which *Brucella* promotes a Warburg-like shift in host cell metabolism by disrupting mitochondrial function.

Brucella abortus **lactate dehydrogenase is required for proper intracellular replication**

Brucella and *Salmonella* both replicate intracellularly and can persist in the host for long periods by shifting host metabolism to make glucose more available (12-14). We measured the growth of *B. abortus* on two preferred substrates, glucose and erythritol, and compared these data to growth on lactic acid. *B. abortus* grows on lactic acid as a sole carbon and energy source as well as it does on glucose or erythritol in standing culture *in vitro* (Figure 4B). We postulated that, during infection, *B. abortus* may exploit the Warburg-type shift in host metabolism by utilizing lactic acid as a carbon and energy source.

To define a genetic determinant of *B. abortus* lactic acid metabolism, we engineered a strain harboring an in-frame deletion of the gene encoding L-lactate dehydrogenase (LDH), *Bab2_0315* (Δ*lldD*). To determine whether *lldD* deletion affects utilization of other carbon sources, we used PM to compare the metabolic activity of Δ*lldD* to wild type (WT), and found that utilization of L-lactic acid was the most statistically significant loss-of-function phenotype (Figure 5A). WT *B. abortus* exhibited robust growth on lactic acid as a carbon and energy source, but Δ*lldD* did not grow in this condition (Figure 5B). The Δ*lldD* mutant had no apparent growth defect in *Brucella* broth supplemented with glucose (Figure 5C), but the numbers of colony forming units (CFU) of Δ*lldD* were significantly reduced in THP-1 macrophages relative to WT at the 48-hour time point (Figure 5D). Complementation of the mutation by introduction of *lldD*

150 at its native locus rescued the THP-1 growth/replication defect. Together, our results
151 indicate that, upon infection, human cells increase lactic acid production and provide an
152 advantage to intracellular *B. abortus*, which can utilize host lactic acid as a carbon and
153 energy source.

154

155 **Small-molecule glycolysis inhibitors inhibit intracellular replication of *Brucella***
156 ***abortus* but do not inhibit axenic growth**

157 Identification of pathogen-induced changes in host metabolism offers new avenues for
158 the development of anti-infectives. Since *Brucella*-infected cells exhibited attenuated
159 mitochondrial function and increased glycolysis, we used small-molecule inhibitors of
160 glucose metabolism (Figure 6A) to determine whether inhibition of the host glycolytic
161 pathway affected intracellular growth/replication of *B. abortus*. We tested: 3-
162 bromopuruvic acid (3-BPA), an inhibitor of energy metabolism that completely
163 eradicated cancer in animal models with no apparent cytotoxicity (15, 16); methyl 1-
164 hydroxy-6-phenyl-4-(trifluoromethyl)-1H-indole-2-carboxylate (NHI-2), a potent
165 anticancer inhibitor of lactate dehydrogenase A (LDH-A) (17, 18); and 2-deoxy-D-
166 glucose (2-dG), a non-metabolizable homolog of D-glucose that slows glycolysis (19).

167 We counted *B. abortus* cells located inside THP-1 cells treated with each of
168 these anti-metabolic compounds at various concentrations. Since some of these
169 compounds may be toxic to cells at the tested concentrations, results were expressed
170 as the number of *Brucella* per THP-1 nucleus; hence, the data represent bacterial

171 counts in live cells only. Each anti-metabolic drug significantly inhibited
172 growth/replication of intracellular *Brucella* in live cells (Figure 6B).

173 To determine whether the antimicrobial activity of these compounds coincides
174 with their cytotoxicity to human cells, we assessed their cytotoxicity using an XTT cell
175 viability assay. As expected, each metabolic inhibitor was cytotoxic at higher
176 concentrations. Treatment of THP-1 cells with 3-BPA, the most potent compound,
177 inhibited *Brucella* infection at non-cytotoxic concentrations. NHI-2 and 2-dG were less
178 potent, but effectively inhibited growth/replication of intracellular *Brucella* (Figure 6C).
179 Both 3-BPA and NHI-2 significantly inhibited intracellular *Brucella* over a range of
180 concentrations that did not affect host cell viability.

181 Finally, to determine whether the antimicrobial effect of these compounds occurs
182 by host targeting, or whether they also directly inhibit bacterial growth, we measured
183 growth and viability of *B. abortus* in axenic culture in the presence of 3-BPA, NHI-2, and
184 2-dG. Neither 3-BPA nor NHI-2 affected growth and viability of *Brucella* in axenic
185 medium, though 2-dG exhibited an inhibitory effect at higher concentrations (≥ 50 mM).

186 These data support a model in which inhibition of host glycolysis and lactate
187 production with 3-BPA and NHI-2 inhibits intracellular *B. abortus* replication without
188 directly targeting *B. abortus* growth (Figure 6D). Together, these results demonstrate
189 that infection-induced changes in host central metabolic pathways are required for
190 proper growth/replication of intracellular *B. abortus*. Inhibition of the glycolytic pathway
191 with host-targeting anti-metabolic compounds provides an effective means to decrease
192 intracellular bacterial load without directly targeting the bacterium (Figure 6E).

DISCUSSION

We have identified metabolic changes in host cells upon exposure to an intracellular bacterial pathogen, *B. abortus*. Intracellular *B. abortus* perturb the morphology and function of host mitochondria, as characterized by loss of the ability to utilize mitochondrial substrates (Figure 1 and 2). The host metabolic effects we observed upon *B. abortus* infection resemble the effect of adding mitochondrial inhibitors (20), and are consistent with the previously reported downregulation of mitochondrion-associated gene expression in macrophages infected with *B. melitensis* (21). Many bacteria are known to target host mitochondria (22), but only a few species have been reported to disrupt mitochondrial morphology (9, 10, 23). The structures of mitochondria observed in our study resemble those of cells treated with uncouplers in combination with a respiration inhibitor; though this treatment resulted in energy deprivation and aggregation of mitochondria, the cells remained viable (24).

Intracellular pathogens compete with the host cell for available nutrients, including central metabolites and amino acids (25). As demonstrated using Biolog mammalian PM, THP-1 cells utilized amino acids as an energy source, but this is inhibited by *B. abortus* infection (Figure 3). The inability of infected cells to utilize amino acids suggests that either intracellular Brucellae compete for the pool of available amino acids, or the cells cease these catabolic reactions because of a change in mitochondrial (or other) physiology. Inhibiting the TCA cycle and increasing glucose metabolism can allow cells to rapidly generate the biomass required for cancer growth. Analogously,

induction of a Warburg-like state upon *B. abortus* infection may enable synthesis of building blocks required for intracellular bacterial growth.

Intracellular pathogens rely on host resources for survival and replication. It is therefore not surprising that other species of bacteria also affect host metabolism upon infection. For example, *Mycobacterium tuberculosis* enhances glycolysis in THP-1 cells (26). Early studies of the infection-induced changes in host metabolism showed that cells infected with *Chlamydia* increase their utilization of glucose through glycolysis and increase lactate production (27). Other pathogens, including the parasite *Plasmodium falciparum* (28), and Mayaro virus (29), also induce similar changes in host metabolism. Because the metabolic changes observed in these hosts are induced upon exposure to various stimuli, it is unlikely that the changes observed in our study are specifically induced by Brucellae.

Erythritol and glucose are preferred energy sources for *Brucella* (30), and our results show that, in axenic culture, *Brucella* can utilize lactate as efficiently as erythritol or glucose (Figure 4). Hence, we hypothesized that intracellular Brucellae can use abundant host lactate as an energy source, which would enable successful intracellular colonization and replication. We took two approaches to test whether host lactate affects intracellular growth. First, we created a lactate dehydrogenase knockout strain Δ*lldD*, which is unable to utilize lactate in axenic culture (Figure 5A-B). While Δ*lldD* showed no growth defects across a range of axenic media, its intracellular replication/survival was attenuated by ~1 log after 48 h in host THP-1 cells (Figure 5D). This suggests that the ability to utilize lactate is necessary for proper replication in the

intracellular niche. We note there are parallels between *B. abortus* pathogenicity and that of intracellular *Neisseria* spp., which is affected by host lactic acid (31). In the second approach, we targeted host lactate synthesis using the small molecule inhibitors NHI-2, 3-BPA, and 2-dG, which decrease lactate levels and inhibit aerobic glycolysis (17, 18, 32, 33). Each of these metabolic inhibitors decreased intracellular growth and/or replication of *Brucella* (Figure 6). Each of these compounds is known for its anticancer properties, but their anti-infective properties were not previously reported. Collectively, the data presented in this study support a model in which intracellular *B. abortus* exploits host metabolic pathways (Figure 7). Hence, the host anti-metabolic compounds identified here and in previous studies (34) may provide a novel therapeutic approach to treat *B. abortus* and other bacterial infections that rely on host metabolic intermediates.

MATERIALS AND METHODS

Bacterial strains

All studies on live *B. abortus* strain 2308 were conducted at Biosafety Level 3 (BSL3) at the Howard Taylor Ricketts Regional Biocontainment Laboratory, University of Chicago, according to US Federal Select Agent Program guidelines. *B. abortus* expressing mCherry was previously generated from the WT *B. abortus* 2308 parent strain by integrating mini-Tn7 expressing a single copy of *mCherry* at the *glmS* locus. Bacterial strains used in this study are listed in Table S1.

258

259 **Mammalian tissue culture**

260 Prior to each experiment, THP-1 macrophage-like cells were grown to a maximum
261 density of 1 x 10^6 mL^{-1} in complete RPMI-1640 medium (HyClone) supplemented with
262 2 mM glutamine (Gibco) and 10% heat-inactivated fetal bovine serum (FBS) (HyClone).
263 HeLa cells were grown in Dulbecco Modified Eagles Medium (DMEM; HyClone)
264 supplemented with 10% heat-inactivated FBS. All tissue culture cells were grown at
265 37°C in a humidified environment with 5% CO_2.

266

267 **Mammalian Phenotype MicroArray: mitochondria toxicity**

268 THP-1 cells were seeded at 50,000 cells/well in two half-area 96-well plates in the
269 presence of 40 ng mL^{-1} phorbol myristate acetate (PMA), and allowed to differentiate
270 for 72 h at 37°C. *B. abortus* 2308 strain was streaked onto Schaedler blood agar (SBA)
271 plates before growing for 2 d, re-streaking, and growing for another 2 d. At the day of
272 infection, *Brucella* cells were scraped off the SBA plate, and suspended and washed in
273 RPMI-1640 growth medium. Cell concentration was measured by the optical density
274 method at 600 nm (OD_{600}). Bacteria were added to the last column of a 96-well plate at
275 1000 MOI, and serially diluted by a factor of two. The first column was left uninfected.
276 Plates were centrifuged at 2170 rpm for 10 min, followed by a 1-h incubation at 37°C
277 and 5% CO_2. Gentamicin was added to each well at a final concentration of
278 100 µg mL^{-1} and the plates were further incubated for 1 h. Following incubation, the

279 medium was removed and replaced with fresh medium containing 25 μg mL^{-1}
280 gentamicin. Cells were incubated for 24 h. Twenty-four hours after infection, two PM-M
281 TOX1 MicroPlates (Biolog) were reconstituted with 50 μL (per well) of MC-0 medium
282 (Biolog IF-M1 medium, 0.3 mM L-Gln, 5% dialyzed FBS, 25 μg mL^{-1} gentamicin). The
283 culture medium was removed from infected cells and replaced with the contents of
284 reconstituted PM-M TOX1 plates. *Brucella*-infected cells were incubated in the presence
285 of mitochondrial substrates for another 24 h. Following this incubation, 10 μL of PM-A
286 dye (Biolog) was added to each well, and the absorbance measured every 15 min (up to
287 150 min) at 590 nm and 750 nm using a Tecan Infinite 200 PRO microplate reader.
288 Plates were incubated at 37°C and 5% CO_2 between readings. The collected
289 absorbance 590 nm data (minus reference absorbance at 750 nm) were analyzed as a
290 function of time.

291 Following the experiment, cell viability was assessed by removing all liquid from
292 the PM-M TOX1 plate, replacing it with glucose-supplemented growth medium
293 containing 10% FBS, and 0.5 mg mL^{-1} MTT reagent, then measuring the absorbance at
294 570 nm after 24 h.

295

296 **Mammalian Phenotype MicroArray: utilization of amino acids**

297 THP-1 and *B. abortus* 2308 cells were prepared as described above. The infection
298 protocol was as described above with small changes. Bacteria were added to
299 differentiated THP-1 cells in a 96-well plate at 100 MOI. Plates were centrifuged at
300 2170 rpm for 10 min followed by 1-h incubation at 37°C and 5% CO_2. Gentamicin was

added to each well at a final concentration of 100 μg mL^{-1} and plates were further incubated for 1 h. Following incubation, the medium was removed and replaced with a fresh medium containing 25 μg mL^{-1} gentamicin. Cells were incubated for 24 h. Twenty-four hours after infection, the content of the mammalian phenotype microarray PM-M2 (Biolog) was reconstituted with 50 μL (per well) of MC-0 medium (Biolog IF-M1 medium, 0.3 mM L-Gln, 5% dialyzed FBS, 25 μg mL^{-1} gentamicin). The culture medium was removed from infected cells and replaced with the contents of reconstituted PM-M2 plates. *Brucella*-infected cells were incubated in the presence of various amino acids for another 24 h. Following this incubation, 10 μL of dye PM-A (Biolog) was added to each well, and the absorbance was measured every 15 min (up to 120 min) at 590 nm and 750 nm using a Tecan Infinite 200 PRO microplate reader. Plates were incubated at 37°C and 5% CO_2 between readings. Absorbance at 590 nm data (minus reference absorbance at 750 nm) was analyzed as a function of time. Results were analyzed by hierarchical clustering using Gene Cluster 3.0 and visualized using Java TreeView (v1.1.6r4).

Bacterial Phenotype MicroArray

Utilization of glucose, erythritol, and lactic acid was measured using PM as previously described (35). Briefly, *B. abortus* strains (WT 2308 and Δ*bab2_0315*) were streaked onto an SBA plate, cultivated at 37°C and 5% CO_2 for 48 h, re-streaked, and grown for another 48 h. Cells were scraped off the plate and resuspended in 1 x IF-0a medium (Biolog) at a final density equivalent to 5% transmittance (OD_{600nm}). PM inoculating

fluids (PM1 and PM2) were prepared from 0.2-µm-filtered and sterilized stock solutions at the following final concentrations: 2 mM $MgCl_2$, 1 mM $CaCl_2$, 25 µM L-arginine, 50 µM L-glutamic acid, 5 µM β-NAD, 25 µM hypoxanthine, 25 µM 5′-UMP, 25 µM L-cystine (pH 8.5), 0.005% yeast extract, and 0.005% Tween 40. PM1 and PM2 inoculating fluids were prepared in 1 x IF-0a GN/GP medium (Biolog). Dye mix G (Biolog) was added to each solution to a final concentration of 1X. A 1:13.6 dilution of 5% transmittance *Brucella* suspension was added to each inoculating fluid. Per well, 100 µL of *Brucella*-containing inoculating fluid was dispensed into each PM plate. PM plates were incubated at 37°C and 5% CO_2, and the absorbance at 630 nm was measured every 24 h for up to 5 d, using a Tecan Infinite 200 PRO microplate reader.

Imaging of mitochondria

HeLa cells were seeded onto 22 x 22 mm cover slides at 50,000 cells/well in a 6-well plate in 2 mL of DMEM medium per well. Cells were grown for 24 h prior to infection. Prior to infection, a culture of *B. abortus* constitutively expressing mCherry was inoculated in *Brucella* broth, and grown overnight at 37°C on orbital shaker. On the day of infection, *Brucella* cells were collected, resuspended in DMEM, and opsonized by incubating for 30 min at 37°C with 1:1000 dilution of serum obtained from *Brucella*-infected mice, as previously described (36). Following opsonization, cells were washed and added to HeLa cells at 10,000 MOI. The plate was centrifuged at 2170 rpm for 20 min, and placed for 24 h at 37°C and 5% CO_2. Following incubation, cells were washed with DMEM, re-infected at 10,000 MOI, and incubated for another 24 h. After

this incubation, cells were washed with DMEM, the cover slide was transferred to a 50 mL tube containing 15 mL DMEM and 200 µg mL^{-1} gentamicin. The slide was incubated at 37°C and 5% CO_2 for 1 h. Following the incubation, 15 µL of 10 mg mL^{-1} Hoechst stain and 2 µL of 1 mM MitoTracker (Molecular Probes) dye were added and incubated for another 20 min. The cover slide was washed and placed on a microscope slide with cells facing up. A drop of DMEM was placed on top of the cover slide and covered by another 22 x 22 mm cover slide. To prevent medium evaporation, the edges were quickly sealed with nail polish, and live cells were immediately imaged using a Leica-DMI6000B fluorescence microscope equipped with a HC PL APO 63X/1.4 NA Oil PH3 CS2 objective. Images were captured using Leica Application Suite X and Hamamatsu Orca-R2 camera.

Quantification of lactic acid

Intracellular lactic acid levels were quantified according to the manufacturer's protocol using a lactate assay kit (Sigma-Aldrich). Briefly, THP-1 cells were seeded and infected with *B. abortus* at increasing MOI, as described above. Infected cells were incubated for 48 h before quantifying lactate levels. After incubation, cells were washed with PBS, homogenized in 60 µL of lactate assay buffer, and cell debris was removed by centrifuging at 14,000 *g* for 10 min. Fifty microliters of supernatant was collected from each sample, and endogenous lactate dehydrogenase was removed by centrifuging supernatants at 14,000 *g* for 30 min using 10 kDa MWCO Ultra-0.5 mL spin filter (Amicon). Twenty microliters of lactate assay buffer was added to each sample to bring the volume up to 50 µL. Fifty microliters of master mix (lactate assay buffer, enzyme

mix, and probe) was added to each well, mixed, and incubated in the dark at room temperature for 30 min before measuring absorbance at 570 nm. Lactate concentration was calculated based on a standard lactate curve and normalized to the number of cells per well.

Construction of *B. abortus lldD* chromosomal deletion

A chromosomal deletion of *B. abortus lldD* (*bab2_0315*) was obtained using a double recombination strategy. Primers used in this study are given in Table S2. The 500 base pairs upstream (using primers 1775 and 1779) and downstream (using primers 1776 and 1777) of *lldD* were Gibson-cloned into pNPTS138, which was digested with *Bam*HI and *Hin*dIII (New England Biolabs). Constructs were validated by DNA sequencing. To delete *lldD*, the deletion plasmid was transformed into *B. abortus*, and primary integrants were selected by plating on SBA supplemented with 50 μg mL^{-1} kanamycin (SBA-Kan). The resulting colonies were grown overnight in *Brucella* broth without selection and plated on SBA supplemented with 5% sucrose to select for second crossovers. The resulting colonies were screened for the *lldD* deletion by sequencing using the sequencing primers 1788/1789.

To complement the *lldD* deletion strain, the *lldD* gene plus the 500 bp upstream and downstream (using primers 1775/1777) were Gibson-cloned into pNPTS138, and restored at the native site using a two-step recombination strategy as outlined above.

Brucella axenic growth

The concentration of *Brucella* cells (WT 2308 and Δ*bab2_0315*) was adjusted to 20% transmittance at OD_{600} and diluted into glucose-containing *Brucella* broth (Difco) at 1:20. MTT (3-(4.5-dimethylthiazol-2-yl)-2.5-diphenyltetrazolium bromide) reagent was added to the media to a final concentration of 0.5 mg mL^{-1}, and cells were continuously incubated at 37°C in a Tecan plate reader, taking absorbance readings at 570 nm every 10 min for 72 h.

Brucella axenic growth: compound cytotoxicity

NHI-2 (Sigma-Aldrich), 3-BPA, and 2-dG (Santa Cruz Biotechnology) were freshly prepared and serially diluted to test concentrations in a half-area 96-well plate in a total volume of 50 µL of PM9 medium (2 mM $MgCl_2$• $6H_20$, 1 mM $CaCl_2$• $2H_2O$, 0.005% yeast extract, 0.005% Tween 40, 2.5 mM D-glucose, 5 mM sodium pyruvate, and 1X Dye Mix G [Biolog]). WT 2308 *Brucella* was prepared from a plate culture in PM9 medium at 20% transmission at 600 nm optical density, and 50 µL was added to each well for a total volume of 100 µL per well. Cells were incubated at 37°C, and absorbance at 630 nm was read every 2 h for 72 h using a Tecan microplate reader.

XTT cell viability assay

The cytotoxicity of NHI-2, 3-BPA, and 2-dG to THP-1 cells was assessed using the XTT cell proliferation and viability assay kit (Roche), according to the supplier's protocol. Briefly, cells were seeded at 50,000 cells/well. Various concentrations of compounds

were added to each well, in triplicate, in the presence of 25 μg mL^{-1} of gentamicin. Cells were incubated for 72 h before measuring viability using the XTT assay. XTT reagents were prepared according to the manufacturer's instructions. Following incubation, 50 μL of XTT labeling mixture was added per well, and cells were further incubated for 4 h at 37°C and 5% CO_2. Absorbance measurements were collected at 590 nm and 750 nm (reference wavelength). Final data were expressed as absorbance readings at 590 nm (minus 750 nm reference absorbance) at the respective compound concentrations.

Quantifying *Brucella* infection of THP-1 cells

THP-1 cells were seeded in a black-well, clear-bottom 96-well plate (Costar) at 50,000 cells/well, differentiated with 40 ng mL^{-1} PMA for 72 h. Two hours before infection, cells were treated with compounds, and infected with *B. abortus* at 100 MOI, as described above. Fresh compounds were added back into media containing 25 μg mL^{-1} gentamicin, and cells were further incubated for 72 h. After incubation, cells were washed three times with 1X PBS, and fixed for 10 min with 4% paraformaldehyde, followed by three washes with 1X PBS. Cell nuclei were labeled with 1 μg mL^{-1} Hoechst stain. Cells were imaged using a Leica-DMI6000B fluorescence microscope equipped with a 20X/0.4 NA objective, Hamamatsu Orca-R2 camera, and Leica Application Suite X. Forty images were captured in four replicate experiments: ten images per condition per replicate. Cell Profiler (v2.1.1) was used to measure the number of intracellular fluorescent Brucellae, and the number of THP-1 nuclei. The effect of the compounds on *B. abortus* intracellular growth was assessed by calculating the number of bacteria per cell, represented as a ratio of the total number of bacteria to the total number of nuclei

(*Brucella* per THP-1 nucleus) per image, which was calculated as an average of 40 images ± standard error of the mean. Statistical significance was determined using one-way analysis of variance (ANOVA) followed by Dunnett's test.

To enumerate CFU at 1, 24, and 48 hours post-infection of THP-1, *B. abortus* cells were resuspended in warmed RPMI and added at a multiplicity of infection (MOI) of 100 CFU per macrophage cell. To synchronize infections after the addition of *Brucella* cells, plates were centrifuged at 200 x *g* for 5 minutes. After a 30-minute incubation, media was removed and replaced with RPMI supplemented with 100 μg mL^{-1} gentamycin to kill extracellular bacteria. Afterwards, samples were incubated for 1 hour, after which monolayers were washed with PBS and THP-1 cells were lysed by addition of 0.01% Triton X-100. Serial dilutions were prepared and viable cells were determined by plating on TSA plates. For longer time points, the RPMI was removed, and replaced with RPMI supplemented with 50 μg mL^{-1} gentamycin. Additional samples were lysed as above and serial dilutions plated. All THP-1 assays were performed in triplicate utilizing independent *B. abortus* cultures.

ACKNOWLEDGEMENTS

We acknowledge the support staff of the Howard Taylor Ricketts Regional Biocontainment Laboratory. We also acknowledge and thank Barry Bochner and Aretha Fiebig for thoughtful feedback and critical evaluation of the manuscript. This study was funded in part by National Institutes of Health grant R01AI107159 to SC, and the

453 Chicago Biomedical Consortium with support from the Searle Funds at the Chicago
454 Community Trust.

455

456 **AUTHOR CONTRIBUTIONS**

457 DC and SC conceived and designed the experiments, analyzed the data, and wrote the
458 manuscript. DC and JW performed the experiments. All authors reviewed and approved
459 the final manuscript.

460

REFERENCES

1. **Galvan-Pena S, O'Neill LA.** 2014. Metabolic reprograming in macrophage polarization. Front Immunol **5:**420.

2. **Pearce EL, Pearce EJ.** 2013. Metabolic pathways in immune cell activation and quiescence. Immunity **38:**633-643.

3. **Kelly B, O'Neill LA.** 2015. Metabolic reprogramming in macrophages and dendritic cells in innate immunity. Cell Res **25:**771-784.

4. **Warburg O, Wind F, Negelein E.** 1927. The metabolism of tumors in the body. J Gen Physiol **8:**519-530.

5. **Bedard K, Krause KH.** 2007. The NOX Family of ROS-Generating NADPH Oxidases: Physiology and Pathophysiology. Physiol Rev **87:**245-313.

6. **Nathan CF, Hibbs JB.** 1991. Role of nitric oxide synthesis in macrophage antimicrobial activity. Curr Opin Immunol **3:**65-70.

7. **Luckhart S, Pakpour N, Giulivi C.** 2015. Host-pathogen interactions in malaria: cross-kingdom signaling and mitochondrial regulation. Curr Opin Immunol **36:**73-79.

8. **Koshiba T.** 2013. Mitochondrial-mediated antiviral immunity. Biochim Biophys Acta **1833:**225-232.

9. **Li T, Xu Y, Liu L, Huang M, Wang Z, Tong Z, Zhang H, Guo F, Chen C.** 2016. *Brucella Melitensis* 16M Regulates the Effect of AIR Domain on Inflammatory Factors, Autophagy, and Apoptosis in Mouse Macrophage through the ROS Signaling Pathway. PLoS One **11:**e0167486.

10. **Stavru F, Bouillaud F, Sartori A, Ricquier D, Cossart P.** 2011. *Listeria monocytogenes* transiently alters mitochondrial dynamics during infection. Proc Natl Acad Sci U S A **108:**3612-3617.

11. **Owen OE, Kalhan SC, Hanson RW.** 2002. The Key Role of Anaplerosis and Cataplerosis for Citric Acid Cycle Function. J Biol Chem **277:**30409-30412.

12. **Xavier MN, Winter MG, Spees AM, den Hartigh AB, Nguyen K, Roux CM, Silva TMA, Atluri VL, Kerrinnes T, Keestra AM, Monack DM, Luciw PA, Eigenheer RA, Bäumler AJ, Santos RL, Tsolis RM.** 2013. PPARγ-Mediated Increase in Glucose Availability Sustains Chronic *Brucella abortus* Infection in Alternatively Activated Macrophages. Cell Host Microbe **14:**159-170.

13. **Roop RM, Caswell CC.** 2013. Bacterial Persistence: Finding the “Sweet Spot”. Cell Host Microbe **14:**119-120.

14. **Eisele NA, Ruby T, Jacobson A, Manzanillo PS, Cox JS, Lam L, Mukundan L, Chawla A, Monack DM.** 2013. *Salmonella* Require the Fatty Acid Regulator PPARδ for the Establishment of a Metabolic Environment Essential for Long-Term Persistence. Cell Host Microbe **14:**171-182.

15. **Cardaci S, Desideri E, Ciriolo MR.** 2012. Targeting aerobic glycolysis: 3-bromopyruvate as a promising anticancer drug. J Bioenerg Biomembr **44:**17-29.

16. **Ko YH, Smith BL, Wang Y, Pomper MG, Rini DA, Torbenson MS, Hullihen J, Pedersen PL.** 2004. Advanced cancers: eradication in all cases using 3-bromopyruvate therapy to deplete ATP. Biochem Biophys Res Comm **324:**269-275.

17. **Granchi C, Calvaresi EC, Tuccinardi T, Paterni I, Macchia M, Martinelli A, Hergenrother PJ, Minutolo F.** 2013. Assessing the differential action on cancer cells of LDH-A inhibitors based on the N-hydroxyindole-2-carboxylate (NHI) and malonic (Mal) scaffolds. Org Biomol Chem **11:**10.1039/c1033ob40870a.

18. **Calvaresi EC, Granchi C, Tuccinardi T, Di Bussolo V, Huigens RW, Lee HY, Palchaudhuri R, Macchia M, Martinelli A, Minutolo F, Hergenrother PJ.** 2013. Dual Targeting of the Warburg Effect with a Glucose-Conjugated Lactate Dehydrogenase Inhibitor. Chembiochem **14:**2263-2267.

19. **Wick AN, Drury DR, Nakada HI, Wolfe JB.** 1957. Localization of the primary metabolic block produced by 2-deoxyglucose. J Biol Chem **224:**963-969.

20. **Bochner BR, Siri M, Huang RH, Noble S, Lei XH, Clemons PA, Wagner BK.** 2011. Assay of the multiple energy-producing pathways of mammalian cells. PLoS One **6:**e18147.

21. **He Y, Reichow S, Ramamoorthy S, Ding X, Lathigra R, Craig JC, Sobral BW, Schurig GG, Sriranganathan N, Boyle SM.** 2006. *Brucella melitensis* triggers time-dependent modulation of apoptosis and down-regulation of mitochondrion-associated gene expression in mouse macrophages. Infect Immun **74:**5035-5046.

22. **Lobet E, Letesson JJ, Arnould T.** 2015. Mitochondria: A target for bacteria. Biochem Pharmacol **94:**173-185.

23. **Ma C, Wickham ME, Guttman JA, Deng W, Walker J, Madsen KL, Jacobson K, Vogl WA, Finlay BB, Vallance BA.** 2006. *Citrobacter rodentium* infection causes both mitochondrial dysfunction and intestinal epithelial barrier disruption

in vivo: role of mitochondrial associated protein (Map). Cell Microbiol **8:**1669-1686.

24. **Lyamzaev KG, Pletjushkina OY, Saprunova VB, Bakeeva LE, Chernyak BV, Skulachev VP.** 2004. Selective elimination of mitochondria from living cells induced by inhibitors of bioenergetic functions. Biochem Soc Trans **32:**1070-1071.

25. **Abu Kwaik Y, Bumann D.** 2015. Host Delivery of Favorite Meals for Intracellular Pathogens. PLoS Pathog **11:**e1004866.

26. **Mehrotra P, Jamwal SV, Saquib N, Sinha N, Siddiqui Z, Manivel V, Chatterjee S, Rao KV.** 2014. Pathogenicity of *Mycobacterium tuberculosis* is expressed by regulating metabolic thresholds of the host macrophage. PLoS Pathog **10:**e1004265.

27. **Moulder JW.** 1970. Glucose Metabolism of L Cells Before and After Infection with *Chlamydia psittaci*. J Bacteriol **104:**1189-1196.

28. **Mehta M, Sonawat HM, Sharma S.** 2005. Malaria parasite-infected erythrocytes inhibit glucose utilization in uninfected red cells. FEBS Letters **579:**6151-6158.

29. **El-Bacha T, Menezes MMT, Azevedo e Silva MC, Sola-Penna M, Da Poian AT.** 2004. Mayaro virus infection alters glucose metabolism in cultured cells through activation of the enzyme 6-phosphofructo 1-kinase. Mol Cell Biochem **266:**191-198.

30. **Anderson JD, Smith H.** 1965. The Metabolism of Erythritol by *Brucella Abortus*. J Gen Microbiol **38:**109-124.

31. **Smith H, Tang CM, Exley RM.** 2007. Effect of Host Lactate on Gonococci and Meningococci: New Concepts on the Role of Metabolites in Pathogenicity. Infect Immun **75:**4190-4198.

32. **El Sayed SM, El-Magd RM, Shishido Y, Chung SP, Diem TH, Sakai T, Watanabe H, Kagami S, Fukui K.** 2012. 3-Bromopyruvate antagonizes effects of lactate and pyruvate, synergizes with citrate and exerts novel anti-glioma effects. J Bioenerg Biomembr **44:**61-79.

33. **Barban S, Schulze HO.** 1961. The Effects of 2-Deoxyglucose on the Growth and Metabolism of Cultured Human Cells. J Biol Chem **236:**1887-1890.

34. **Czyz DM, Jain-Gupta N, Shuman HA, Crosson S.** 2016. A dual-targeting approach to inhibit Brucella abortus replication in human cells. Sci Rep **6:**35835.

35. **Herrou J, Czyż DM, Willett JW, Kim HS, Chhor G, Babnigg G, Kim Y, Crosson S.** 2016. WrpA Is an Atypical Flavodoxin Family Protein under Regulatory Control of the *Brucella abortus* General Stress Response System. J Bacteriol **198:**1281-1293.

36. **Kim HS, Caswell CC, Foreman R, Roop RM, Crosson S.** 2013. The *Brucella abortus* General Stress Response System Regulates Chronic Mammalian Infection and Is Controlled by Phosphorylation and Proteolysis. J Biol Chem **288:**13906-13916.

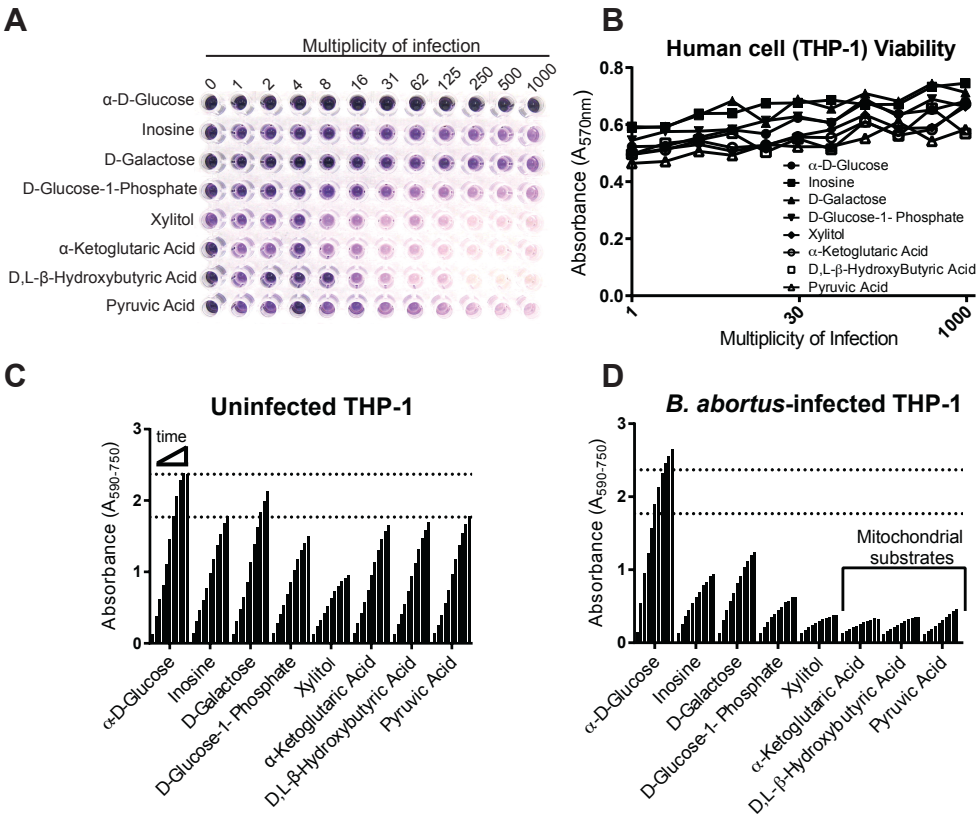

572

573 **FIG 1. Mitochondrial function is perturbed in THP-1 cells infected with *B. abortus*.**

574 **(A)** Mammalian Phenotype MicroArray (PM) plate designed to measure mitochondrial
575 function. The ability of THP-1 cells infected with *B. abortus* at increasing multiplicity of
576 infection (MOI) to utilize metabolic substrates was assessed by measuring the reduction
577 of a tetrazolium dye (see Materials and Methods). **(B)** An MTT cell viability assay was
578 performed in the presence of glucose to assess the effect of *B. abortus* infection on
579 human cell survival at the conclusion of the mammalian PM assay. Dye reduction by **(C)**
580 uninfected and **(D)** *Brucella*-infected human cells (MOI 125) measured as a time-
581 dependent absorbance readout. Cells were cultured in minimal medium supplemented
582 either with glucose (control) or central metabolic substrates. Brackets indicate
583 substrates (α-ketoglutaric acid, β-hydroxybutyric acid, and pyruvic acid), which enter the

584 mitochondria, thereby providing a direct readout of mitochondrial function. Bars along
585 the X axes represent time (0–150 min) in 15-min increments. Dotted lines mark the
586 highest reading for utilization of glucose and pyruvic acid in uninfected THP-1 cells.

587

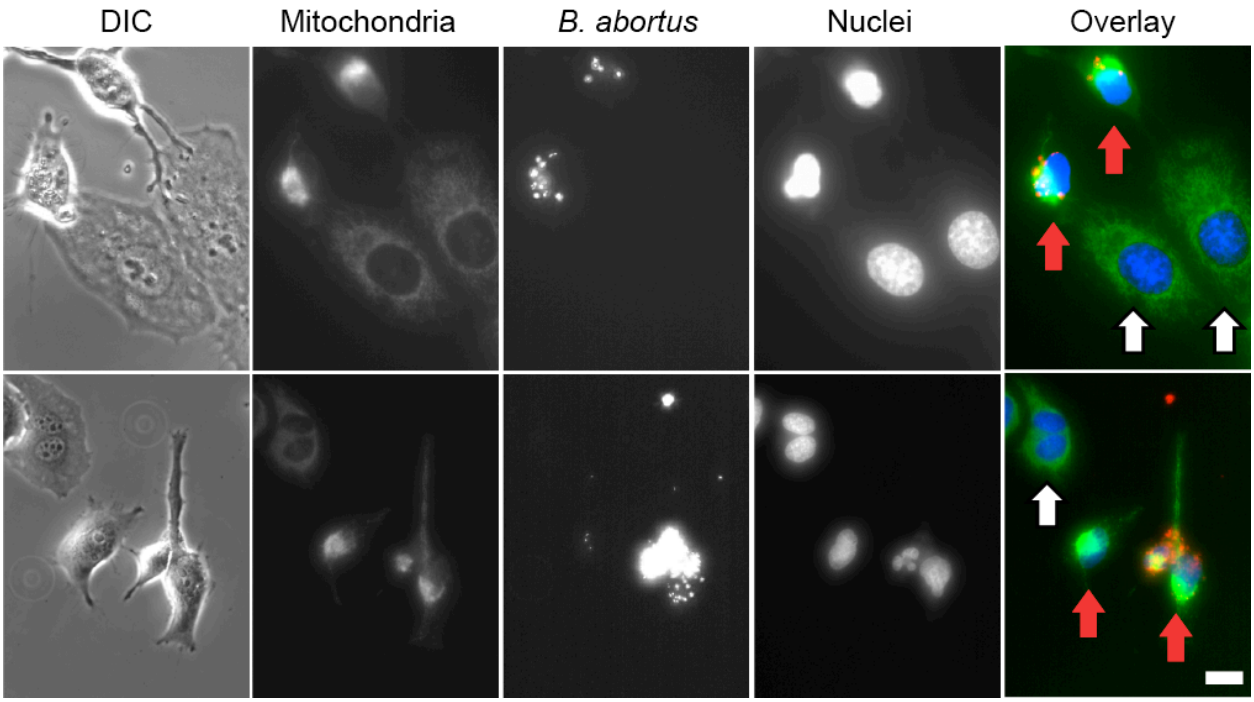

FIG 2. Intracellular *B. abortus* induces morphological changes of mitochondria in HeLa cells.

Two fields showing mitochondrial staining (MitoTracker, green), *B. abortus*-Tn7mCherry (mCherry fluorescence, red), nuclei (Hoechst stain, blue), and the corresponding image with differential interference contrast (DIC) microscopy. Red arrows indicate cells with visible intracellular *B. abortus*, white arrows indicate cells for which no infection is evident. Cells not infected with *B. abortus* have typical morphology and mitochondrial structure. Scale bar = 50 µm.

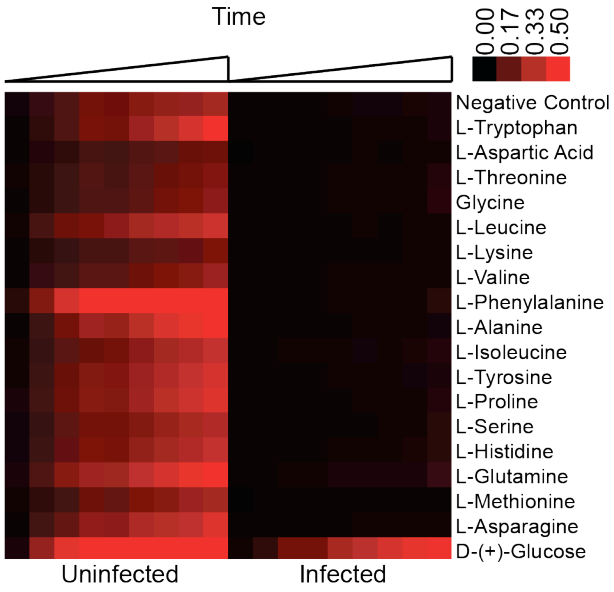

FIG 3. Host cell utilization of amino acids as a carbon source before and after *B. abortus* infection.

Heatmap representing host cell metabolism as measured colorimetrically via a redox dye (see Materials and Methods). Time-dependent metabolic change of non-infected versus *B. abortus*-infected THP-1 cells in the presence of amino acids are plotted. Color is an arbitrary scale from black (no reduction of the dye, 0.00) to red (maximum reduction of the dye, 0.50).

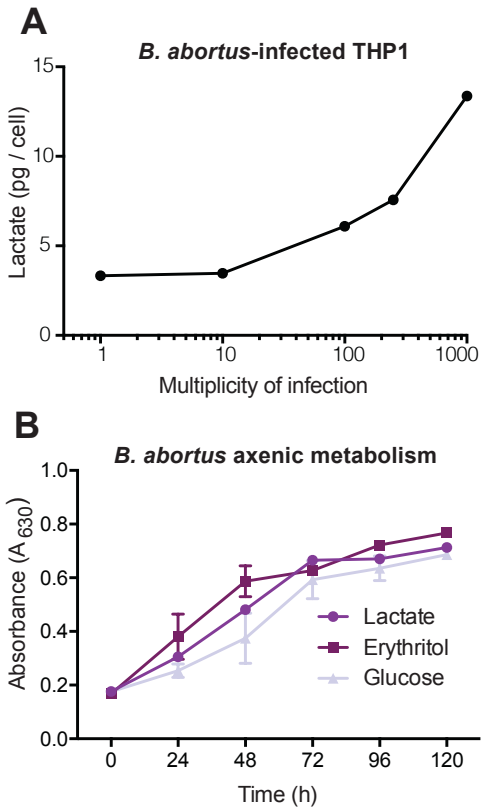

607

608 **FIG 4. *B. abortus* induces host cell lactate production and utilizes lactate as a**
609 **carbon and energy source as efficiently as glucose and erythritol.**

610 **(A)** Lactate levels in THP-1 cells upon infection with *B. abortus* at different multiplicities
611 of infection. **(B)** Metabolism of *B. abortus* measured on carbon/energy sources lactate,
612 erythritol, or glucose. Data show an average of two independent experiments ±
613 standard deviation.

614

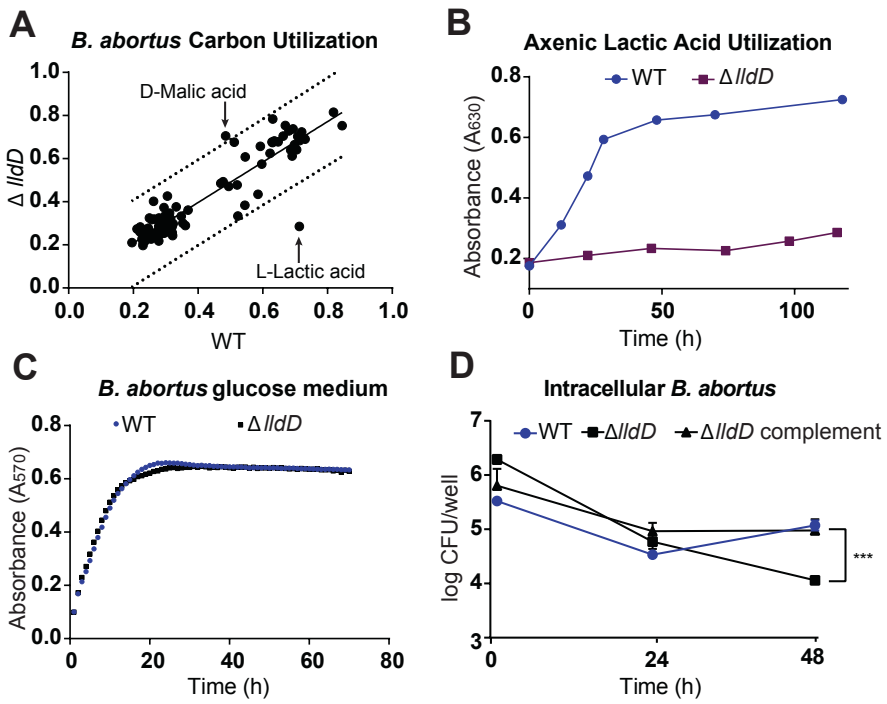

615

616 **FIG 5. *B. abortus* L-lactate dehydrogenase deletion strain Δ*lldD* cannot utilize**
617 **lactic acid in axenic culture and is attenuated in a macrophage infection model.**

618 **(A)** Phenotype MicroArray carbon utilization measurements of wild-type (WT) *B. abortus*
619 and L-lactate dehydrogenase (LDH) mutant (Δ*lldD*) strains. Metabolic activities for
620 growth on 95 distinct carbon substrates (see Materials and Methods) are plotted against
621 each other; the dotted line marks a 99% prediction band of a linear regression.
622 Correlation values above the line represent a gain-of-function phenotype and values
623 below the line represent a loss-of-function phenotype. L-lactic acid and D-malic acid are
624 marked as loss-of-function and gain-of-function, respectively **(B)** Graph representing
625 time-dependent utilization of lactic acid as a carbon energy source, and measured by a
626 metabolic indicator dye (see Materials and Methods). **(C)** Graph representing axenic
627 growth of the WT and Δ*lldD* strains in glucose-containing *Brucella* broth. **(D)** Intracellular

628 replication of the WT and Δ*lldD* strains in macrophage cell infection model. Intracellular
629 Brucellae were quantified as $\log_{10}$ colony forming units (CFU) per well at 1, 24, and 48 h
630 post-infection. Lines represent WT (●), Δ*lldD* mutant (■), and complement (▲). n=3,
631 Error bars represent standard deviation.

632

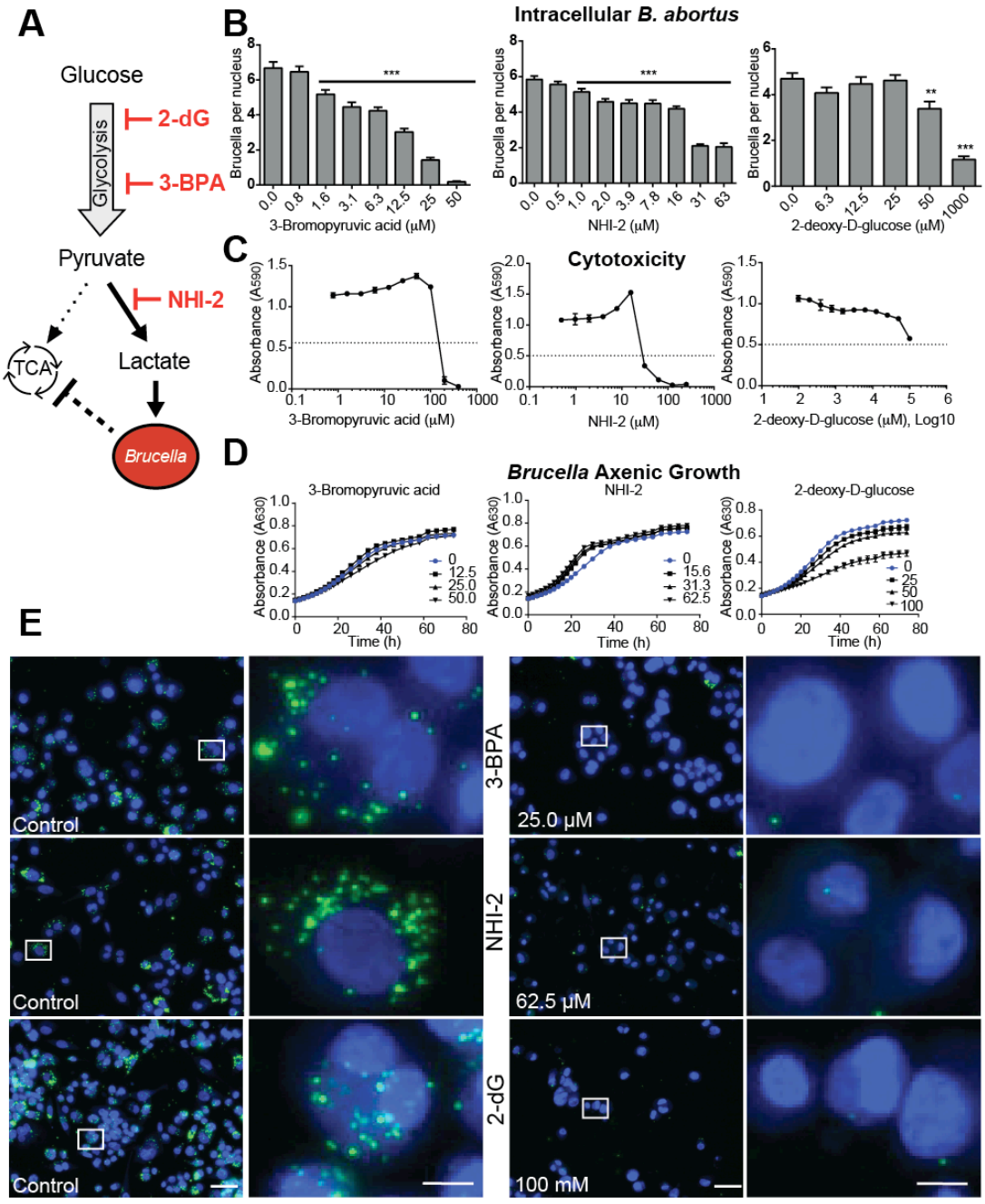

633

634 **FIG 6. Pharmacological disruption of the host glycolytic pathway and lactate**

635 **production inhibits replication of intracellular *B. abortus*.**

(A) Model depicting *Brucella*-dependent modulation of carbon metabolism and activation of aerobic glycolysis, resulting in the production of lactate. *B. abortus* utilizes lactate as efficiently as preferred substrates glucose and erythritol. Pharmacological inhibitors of glycolysis, 3-Bromopyruvic acid (3-BPA), NHI-2, and 2-deoxy-D-glucose (2-dG), inhibit intracellular growth of *B. abortus*: **(B)** Graphs represent the effect of 3-BPA, NHI-2, and 2-dG on intracellular replication of *B. abortus* as quantified by enumerating fluorescent bacteria per THP-1 nucleus; **(C)** cytotoxicity of inhibitory compounds to THP-1 cells, and **(D)** effect of metabolic inhibitors on *B. abortus* axenic growth/metabolism. The effect of anti-glycolytic compounds on infection was assessed by measuring the average ratio of bacteria-to-nuclei in THP-1 cells treated with each of the compounds. Statistical significance was evaluated from four biological replicates (10 images each) using one-way analysis of variance (ANOVA) followed by Dunnett's post test $^{**}p< 0.01$, $^{***}p<0.0001$). Error bars represent ± standard deviation from the mean; an XTT assay was used to measure compound cytotoxicity to THP-1 cells; *Brucella* axenic growth/metabolism was assayed by measuring tetrazolium-based dye reduction at 630 nm **(E)** Fluorescence images of nuclei (blue) and intracellular *B. abortus* (pseudocolored green) reflect the efficacy of 3-BPA, NHI-2, and 2-dG to inhibit *B. abortus* replication in the intracellular niche. Scale bars = 10 μm (full view) and 50 μm (magnified insets, marked with white box in full view). Dotted line = half maximal inhibitory concentration (IC50).

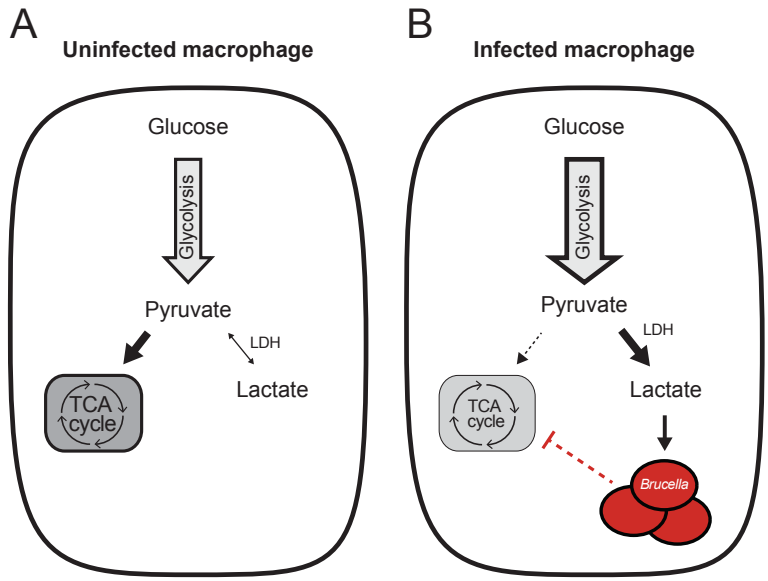

FIG 7. Model of how *B. abortus* exploits the shift to Warburg-like metabolism in macrophages.

Data presented in this study support a model in which inhibition of tricarboxylic acid (TCA) cycle metabolism upon infection biases the host cell toward the production of lactic acid. **(A)** Uninfected macrophages exhibit typical central carbon metabolism in which pyruvate enters the TCA cycle. **(B)** *B. abortus* infection biases the macrophage toward aerobic glycolysis and lactate production. *B. abortus* efficiently utilizes lactic acid via the lactate dehydrogenase (LDH) enzyme, LldD. A strain lacking *lldD* is compromised in axenic lactic acid metabolism and in intracellular replication in a THP-1 macrophage model. Pharmacological inhibition of host glycolysis or LDH-A inhibits *B. abortus* replication.